JOURNAL OF MATERIALS SCIENCE 6 (1971) 509–530

Deformation of Polyoxymethylene by Rolling

D. M. GEZOVICH, P. H. GEIL
Division of Macromolecular Science, Case Western Reserve University, Cleveland, Ohio 44106, USA

The deformation due to rolling of polyoxymethylene (POM) was investigated by using wide and small angle X-ray techniques and electron microscopy. Tensile tests of rolled POM indicate that the yield stress increases along the roll direction. This is accompanied by a decrease in the yield stress perpendicular to the roll direction. Wide angle X-ray data from uniaxially rolled POM, obtained by means of pole figures, indicate that molecular chains tilt preferentially at approximately 30° to the roll direction at low rolling deformation, and align in the roll direction when the sample is rolled to its fullest extent. A lamellar tilt of of about 30° is also observed. Thus, the chains must tilt within the lamellae. When samples are fully rolled, small angle patterns indicate at least partial breakup of lamellae. Biaxial rolling produces no such breakup, but a uniform tilting of lamellae through the entire range of deformation.

1. Introduction

Cold-rolling has, for some time, been an important forming process for metals; the cold working produces an improvement in the tensile properties of the resulting sheets and rod-like forms. Likewise cold-rolling can be used to form polymers with improved properties. Being a continuous process and producing, as shown here, unique, oriented morphological structures, it is anticipated that cold-rolling will play an increasingly important role in polymer technology. The purpose of this paper is to show the structural changes which occur during the rolling process in polyoxymethylene (POM) and to discuss the physical properties that these changes influence.

A complete and unambiguous description of the orientation in polymers caused by rolling requires X-ray pole figures (i.e. a two-dimensional representation of a spherical distribution of plane normals with respect to known sample directions, in this case roll direction, RD; transverse direction, TD; and thickness, TH). A pole figure can describe orientation either on the molecular level, i.e. orientation of a lattice plane, or on the lamellar ($\sim$ 100 Å) level. In the latter case, small angle X-ray diffraction (SAXD) techniques are used, rather than the wide angle X-ray diffraction (WAXD) methods normally reported. The pole figure is then a plot of lamella normals.

At the very least, three X-ray patterns along three mutually perpendicular directions are needed to describe the texture on either the lamellar or molecular level. From this, a simplified pole figure can sometimes be determined. This is the method used by Hay and Keller [1, 2] in their study of orientation in drawn and rolled polyethylene, the only polymer for which detailed studies of the deformation process during rolling have been reported.

Hay and Keller [1, 2] and Frank, Keller, and O'Connor [3] reported that mild rolling of polyethylene leads to an orientation where the (1 0 0) planes are parallel to the plane of the film and the [0 0 1] direction is parallel to the direction of advance (roll direction). However, the orientation is poorly defined in mildly rolled samples. With increased rolling, this orientation becomes better defined and in addition a second orientation appears with (1 1 0) planes parallel to the film plane. The latter becomes more pronounced with stronger rolling. The authors [1-3] suggest (3 1 0) and/or (1 1 0) twinning when polyethylene is rolled and that rolling can be regarded as nearly the same as transverse compression. The twinning can subsequently be removed by appropriate heat treatment and a

"single-crystal" orientation with respect to both unit cell and supermolecular structure can be obtained [4].

Cold-rolled polypropylene has been shown to exhibit a preferred *c*-axis orientation inclined at a small angle to the roll direction [5, 6]. The orientation in the roll direction is stronger for more severe rolling, and the angle of inclination from the roll direction is smaller (being about 10° for a sample cold-rolled to $\frac{1}{6}$ of its initial thickness). Wilchinsky suggested that the tensile component of force along the roll direction produces a local partial necking within the sample [5].

Accompanying the molecular orientation in rolled polymers is a rearrangement of supermolecular order. In many rolled polymers a so-called SAXD four-point pattern is found [2, 4]. The origin of this type of pattern, which is also found in oriented polymer systems produced by drawing, has been the subject of much discussion [2, 7-10]. Several models have been proposed to explain this pattern. A number of years ago Statton [11] and Hess and Kiessig [12] suggested a model consisting of ordered (crystalline), and disordered ("amorphous") regions alternating more or less regularly. Models [10, 13, 14] have also been suggested which rely on particle scattering of individual fibrils. Recently, other models for drawn polymers have been suggested based on possible lamellar structures. The four-point pattern is assumed to arise from two distinct lamellar orientations, each giving rise to two of the four lobes of the pattern [2, 15]. Seto and Tajima [16] use this model to explain the four-point pattern obtained by compressing fibres of polyethylene along their axes. A similar model, proposed by Bonart [17], consists of a paracrystalline layer lattice with the layers lying obliquely.

As one would expect, the structural changes during rolling have a substantial effect on physical properties. Because of the anisotropic nature of the rolling process, properties such as tensile strength, elastic modulus, brittle strength, dielectric strength and others depend on the direction of measurement with respect to the roll direction. However, polymers rolled first in one direction and then in a direction perpendicular to the first roll are, in general, not as dependent on direction as those rolled only in one direction [18-20]. When annealed at temperatures above the rolling temperature but below T_m, the properties (and orientation) of the rolled samples in some cases revert toward those of unrolled samples [2, 21, 22] whereas in others [18] they do not.

The effect of rolling on physical properties has been reported for such polymer systems as polyethylene [20, 23], polypropylene [18], polyoxymethylene [19], polyvinylidene fluoride [24], polycarbonates [21, 25] and acrylonitrile-butadiene-styrenes ter-polymers [25]. Similar results were found for all of these materials. As a result of rolling, the tensile strength in the direction of rolling increased and yielding became less evident. In many cases the rolled samples deformed by uniform extension. In the transverse direction the strength decreased slightly and the elongation increased relative to that along the roll direction. (Rolled polyoxymethylene responds in a somewhat different manner with regard to elongation to break. This fact will be discussed later). The increase in strength for biaxially rolled specimens was less than that of the uniaxially rolled material. Accompanying these changes in tensile properties was a decrease indensity (for polyethylene [20]). This decrease is attributed to both destruction of crystal structure and void formation.

2. Experimental

2.1. Preparation of Samples

POM samples for X-ray analysis were prepared by rolling injection moulded bars of Celcon* through a 3 in. diameter mill, at room temperature. The bars, initialy 0.123 in. thick. were reduced in thickness 0.005 in. per pass to a minimum thickness of 0.080 in. They were then reduced 0.002 in. per pass, until the desired thickness was achieved. Broutman and Kalpakjian [25] reported a temperature increase of about 20°C (from 25°C) for polycarbonate subjected to cold rolling under similar conditions as those described here. Such an increase would not introduce serious annealing effects in a polymer such as POM(T_m = 162°C). The bars were rolled slowly (approximately 1 in./sec) and set aside for several minutes after each pass in order to minimise even these heating effects. For "uniaxially" rolled samples, the bars were passed through the mill in the same direction each time. "Biaxially" rolled samples were passed through the mill in one direction and then in a direction perpendicular to the first pass. This process was repeated, each time reducing the

*Celanese trade mark.

thickness by 0.005 in., until the desired thickness was achieved. The initial thickness is defined as L_0, the thickness after rolling is L, and the ratio L/L_0 is the "extent of roll". WAXD and SAXD indicated that little or no initial orientation was present. Selected samples were annealed in glycerin at the desired temperature for 1 h.

2.2. Tensile Tests

The stress-strain curves were obtained at room temperature using an Instron tensile testing instrument with a strain rate of 0.05 in./min (about 6% strain/min). Dumbbell shaped tensile specimens (gauge length = 0.85 in.) were cut from the rolled sheet at various angles to the roll direction in order to investigate the anisotropy of the material.

2.3. X-ray Examination

WAXD flat plate photographs were obtained on a Rigaku-Denki unit using CuK_α radiation. WAXD pole figures were obtained on an automated Picker 4-angle, full circle goniostat with computerised plotting of the data. POM has a 9_5 helix conformation and packs in a hexagonal unit cell. $10\bar{1}0$ (equatorial) and $10\bar{1}5$ (quadrant) were mapped over one-half of a hemisphere in a manner similar to that described by O'Leary and Geil [7]. A background count was also made at each orientation. Intensity data taken from an unoriented sample of similar size using the above technique, showed that absorption corrections were negligible.

SAXD photographs were taken on a Rigaku-Denki rotating anode SAXD unit using CuK_α radiation. In order to obtain patterns at various positions with respect to sample thickness, the sample was placed on a goniometer which was capable of translation perpendicular to the main beam.

The Rigaku-Denki SAXD diffractometer was also used for SAXD pole figure data using a physical set up similar to that described by Cullity [26]. 0.3 mm point collimation was used with samples approximately 1 × 1 × 5 mm in size. Data were taken every 10° and a 100 sec count time was used. However, in regions of high intensity or where intensity was changing rapidly, data were taken every 5° in order to ascertain more accurately the size and shape of the maxima. The diffractometer was set at the peak maximum in 2θ and the samples rotated manually to obtain all possible orientations of the sample. Intensity data taken from an unoriented sample of the same size showed that absorption corrections were again negligible. Scans over 2θ were taken at several sample positions to determine whether the small angle spacings depended on sample orientation. The peak position in 2θ was found to be independent of sample orientation for unannealed specimens with L/L_0 greater than 0.5; exceptions for other samples will be discussed in the test. This method has been described in detail elsewhere [4, 27].

2.4. Electron Microscopy

Fracture surfaces were prepared for electron microscopy using samples of Delrin* which were originally compression moulded and slow cooled from the melt, rolled in the manner described previously and fractured in liquid nitrogen. The surfaces were replicated in the usual manner using Pt-C evaporation and polyacrylic acid to remove the replicas. Small angle photographs were taken from the same areas in order to correlate the small angle patterns with the micrographs. These samples had a small angle spacing of 193 Å as compared with a spacing of 177 Å in the injection moulded bars of Celcon. Slow cooling resulted in fractured samples which yielded clearer micrographs; micrographs of the fractured Celcon were similar to those reported here.

3. Experimental Results

3.1. Tensile Tests

Stress-strain data from rolled POM indicates that an improvement of tensile properties occurs when the test specimens are cut parallel to the roll direction. This improvement is accompanied by a decrease of tensile strength in the transverse direction. Fig. 1 shows typical stress-strain curves for POM rolled to $L/L_0 = 0.77$, 0.59 and 0.42 respectively. θ is the angle between the tensile specimens and the roll direction. The dashed lines indicate the ranges over which the samples broke. In each case the dotted line represents the "as moulded" sample. The "as moulded" material always broke immediately after yielding occurred.

Up to an extent of roll of about 0.4, as θ decreases from 90° to 0°, i.e. as the tensile specimens are cut at a smaller angle to the roll direction, both the stress to break and strain to break tend to increase (fig. 1a, b). However, this

*Dupont trade mark.

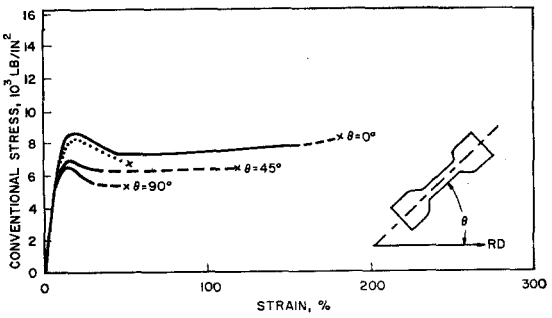

Figure 1 Typical stress-strain curves for L/L_0 0.77, 0.59, and 0.42.

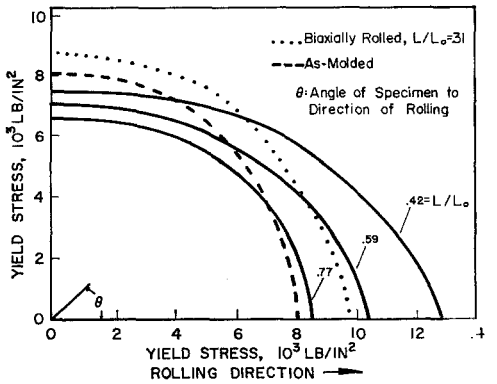

Figure 2 Polar plot showing the asymmetry of yield properties of rolled POM.

was not true for the highly deformed material (fig. 1c). In this case the samples cut parallel to the roll direction broke at a lower strain than those with $\theta = 0$. This behaviour occurred in all samples where the molecular axis was found by X-ray diffraction (described later) to be nearly parallel to the roll direction.

One further point should be made concerning the elongation to break in these samples. The variation in elongation for which a sample will break is small for $\theta = 0$, because the sample yields, necks and then line draws until it is fully extended and finally breaks. However, as θ is increased, the samples tend to break, subsequent to yielding, at various elongations and seldom reach full extension. In general, this variation increases as θ increases.

The variation of strain at break with θ is notably different from that which has been reported for other polymers, including polyethylene [23] and polypropylene [18]. These polymers break at lower elongations when the tensile specimen is cut parallel to the roll direction. In many cases deformation prior to failure is uniform for $\theta = 0$. However, for POM, yielding always occurs and is sharper and better defined as θ approaches 90°.

Fig. 2 is a polar plot with θ as the angular variable and yield stress as the radial variable. This plot is a summary of the data and shows the degree of anisotropy found in uniaxially rolled POM. For reference the "as-moulded" material is shown as a dashed line. The yield stress for biaxially rolled specimens, $L/L_0 = 0.31$ (dotted line), was 13 to 22% greater than that of the "as-moulded" material, and nearly independent of the angle between the rolling direction and tensile specimen.

3.2. Dimensional Changes

The dimensional changes which occur in POM with uniaxial rolling are shown in fig. 3. Note that up to a 40% increase in width of the samples can be observed, indicating that a substantial amount of deformation is occurring in the transverse direction.

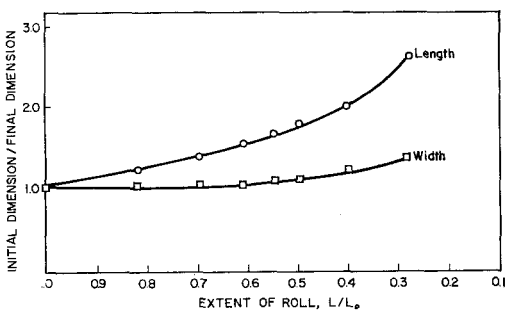

Figure 3 Macroscopic dimensional changes due to rolling.

3.3 X-ray Diffraction

3.3.1. Uniaxial Rolling

WAXD flat plate photographs of POM were taken along three mutually perpendicular axes for several extents of roll. In samples with L/L_0 between 0.9 and 0.5 little orientation of the patterns can be observed. At a deformation ratio of 0.4 or less the patterns are similar to those from a drawn fibre. However, maxima in the $(10\bar{1}0)$ Debye-Sherrer ring occur on the meridian of the pattern, when the beam is parallel to the transverse direction, which cannot be explained in terms of a fibre pattern. These maxima occur at all extents of roll and will be discussed later.

Because these patterns are quite complex and

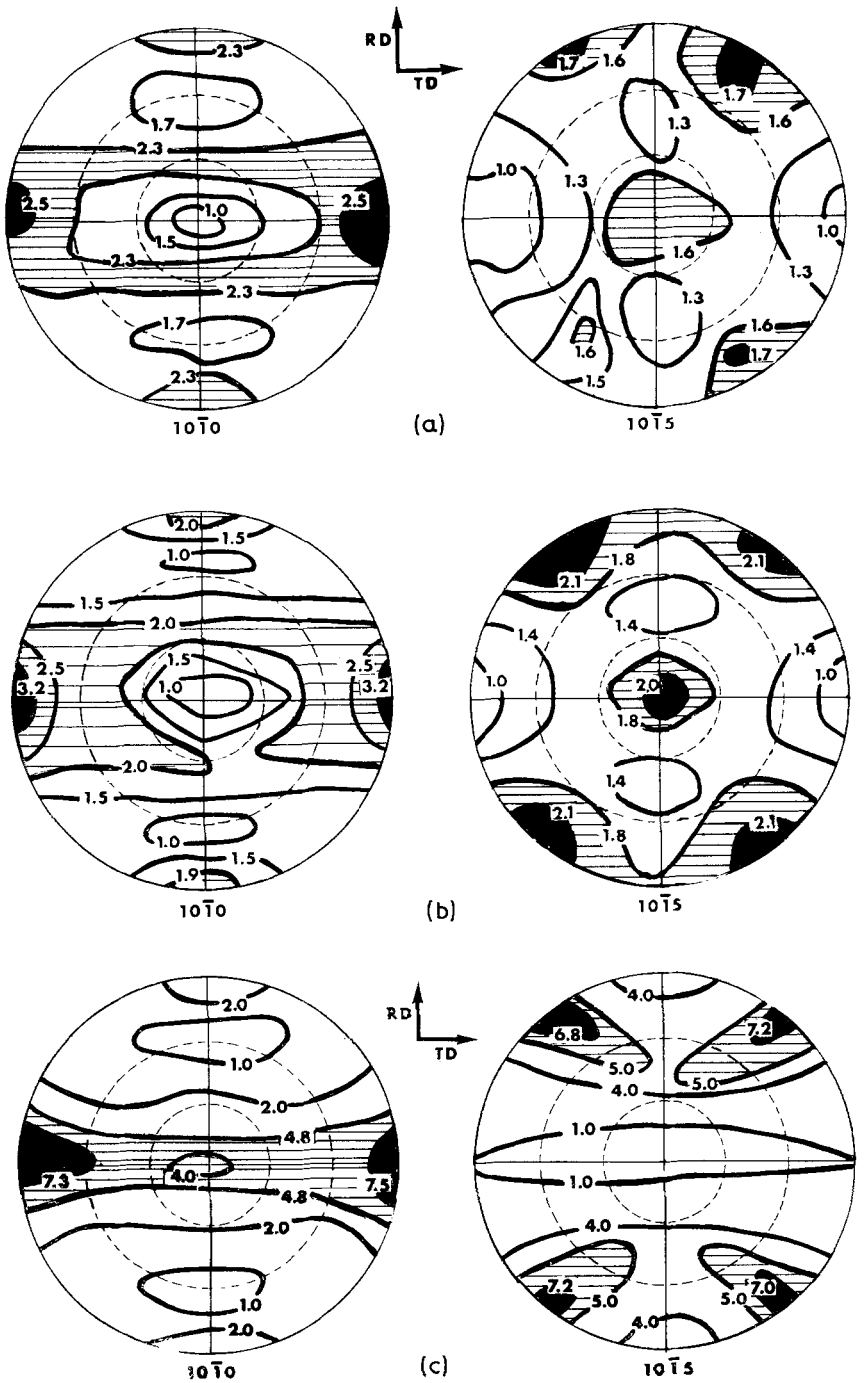

Figure 4 WAXD pole figures as a function of L/L_0 (a) $L/L_0 = 0.7$. (b) $L/L_0 = 0.5$. (c) $L/L_0 = 0.28$.

difficult to analyse unambiguously, a three-dimensional representation of the orientation was desirable. Fig. 4 shows the WAXD pole figures of rolled POM as a function of extent of roll. The distributions of the poles of two reflections were measured: (10$\bar{1}$0), whose poles are perpendicular to the molecular axis and (10$\bar{1}$5), whose poles are at 42° to the molecular axis. The general shape of the figure does not change as L/L_0 decreases from 0.9 to 0.5. However, the maxima

become sharper and relatively more intense at the higher deformations. The patterns for the $(10\bar{1}0)$ reflection at low deformations consist of two bands on either side of the equator and secondary maxima at the north and south (RD) poles. The $(10\bar{1}5)$ reflection has four maxima along the outer circumference at about 30 to 40° from the roll direction and an equally intense maximum in the centre. At an extent of roll of 0.4 to 0.5, the figure changes suddenly to that shown in fig. 4c. This is very nearly the pattern obtained from a fully drawn fibre, indicating a c-axis orientation nearly parallel to the roll direction. However, even in the fully rolled sample, the crystal orientation about the roll direction is not uniform, as indicated by the minima in the bands of intensity (fig. 4c). (A fibre pole figure would have uniform intensity in the equatorial $(10\bar{1}0)$ band and the two $(10\bar{1}5)$ bands.) Furthermore, the weak $10\bar{1}0$ maxima along the roll direction in fig. 4c cannot be explained in terms of a fibre pattern. These extraneous $(10\bar{1}0)$ maxima occur in all of the figures, and corresponding to the meridional maxima in the WAXD patterns mentioned above.

The pole figures of POM samples of low rolling deformation are obviously more complex and difficult to interpret than those of samples which are fully rolled. One way to approach such a problem is to assume a certain crystalline texture and construct the appropriate pole figure for comparison with the observed data. Fig. 5 shows the calculated $(10\bar{1}0)$ and $(10\bar{1}5)$ pole figures for the case in which the c-axis (molecular axes) are assumed inclined at an angle of $\pm 30°$ to the roll direction, out of the roll (RD-TD) plane, and the crystals allowed to rotate about these axes. Strong maxima occur where the two resulting bands overlap. The result agrees well with the major observed intensity. The maxima which occur at the north and south poles in the $(10\bar{1}0)$ pole figures indicate the presence of additional chains which are perpendicular to the roll direction. Because of the complexity of the figures, it is difficult to tell whether these chains are parallel to the transverse direction, or positioned in some other manner in the TH-TD plane. (This will be discussed later in terms of SAXD.) The maximum at the centre of the $(10\bar{1}5)$ pole figures can be explained in terms of the overlap of the tails of the two bands centred in the hemisphere shown in fig. 5 and/or the presence of chains perpendicular to the roll direction.

In order to determine how the lamellae (crystallites) deform with respect to the molecular chains in cold rolled POM, SAXD photographs were taken. Fig. 6 shows small angle photographs as a function of extent of roll along three mutually perpendicular directions. These data are presented in tabular form in table I.

The dominant feature of the SAXD patterns is the presence of a well defined and relatively intense four-point pattern when the beam is in the transverse direction. For future reference, the angle β is defined as the angle between the lobes in the four-point pattern and including the

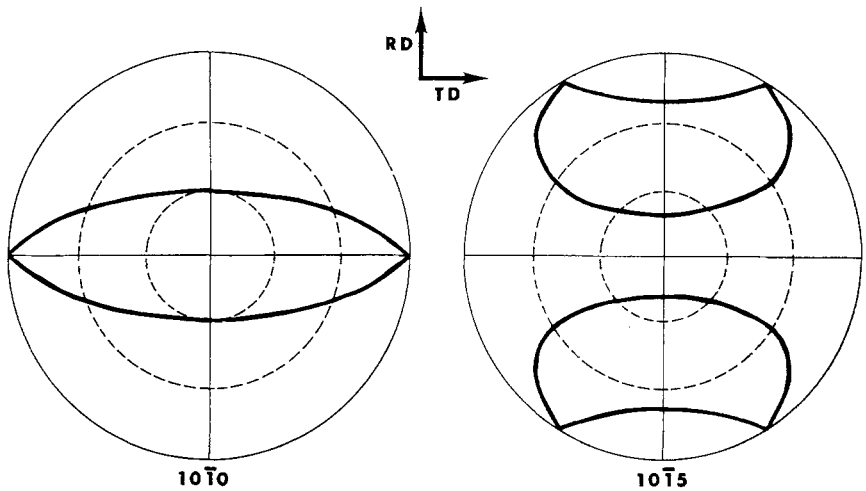

Figure 5 Calculated $10\bar{1}0$ and $10\bar{1}5$ pole figures for uniaxial rolling.

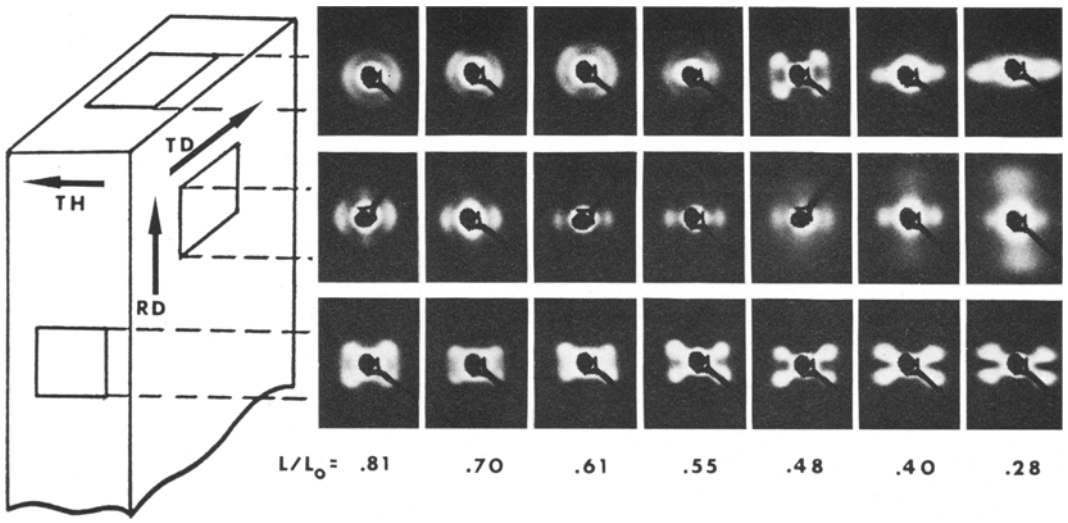

Figure 6 SAXD photographs of uniaxially rolled POM as a function of L/L_0.

TH direction (table I). Assuming, as shown later, that the SAXD pattern arises from lamellae, then β is twice the angle between the lamellae and the roll direction. The angle β decreases steadily as L/L_0 decreases, while the measured long period decreases until L/L_0 reaches a value of about 0.5 as shown in fig. 7. Further, the lobes of the four-point patterns become better defined and more intense as L/L_0 is decreased. At $L/L_0 = 0.5$ the spacing rapidly decreases to a value of about 140 Å and the shape of the lobes changes.

When viewed along the rolling direction, the patterns, at low rolling deformations consist of two arcs, suggesting a periodicity along the thickness direction. As L/L_0 is decreased from 0.8 to 0.6, the arcs intensify at the ends and split into a four-point pattern. The angle between the lobes of this four-point pattern is defined as α in

TABLE I Observed small angle spacings for uniaxially rolled POM

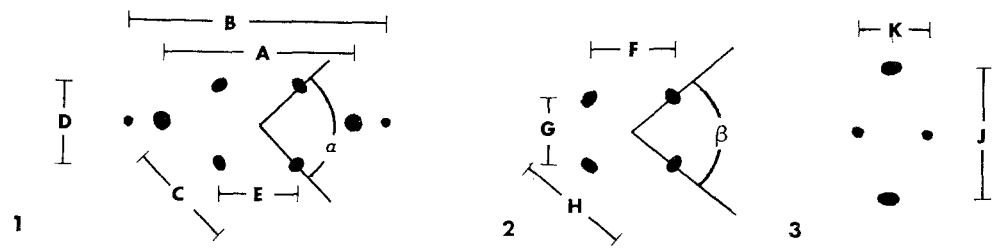

L/L_0	A	B	C	D	E	α	F	G	H	β	J	K
0.81	—	—	167 (arc)	—	—	—	216	264	171	78°	165	168 (arc)
0.70	—	—	165 (arc)	—	—	(116°)	196	279	165	69°	156 (w)	165
0.61	—	—	163	—	—	(107°)	189	317	163	62°	—	162
0.55	—	—	162	265	216	92°	188	322	160	61°	—	163
0.48	—	—	160	274	220	79°	187	321	163	59°	—	158
0.40	138	w	141 (w)	(w)	(w)	—	156	320	141	50°	109	159
0.28	137	69	144 (w)	(w)	(w)	—	156	343	139°	48°	105	162

(w = weak reflection)
Columns 1, 2, and 3 correspond to the patterns in fig. 6 with the beam in the RD, TD and TH directions respectively. The subcolumns A-K list Bragg spacings calculated from the reflections as defined in the sample patterns at the top of the columns; greek letters refer to the angles shown.

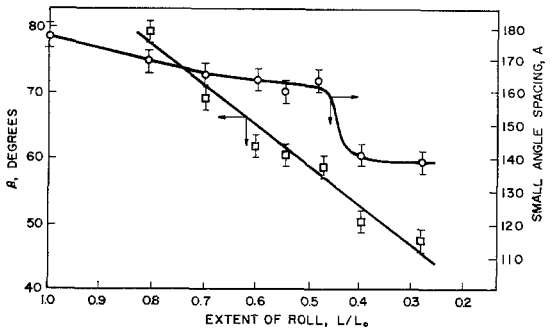

Figure 7 Effect of uniaxial rolling on lamellar tilt and small angle spacing.

table I. At an extent of roll of about 0.4, the four-point pattern nearly disappears and a strong, well defined periodicity again appears along the thickness direction. Traces of the four-point pattern, however, can be seen even when the sample is rolled the maximum amount possible.

The small angle patterns obtained with the beam parallel to the thickness direction also show interesting orientation effects. At first glance, the patterns at low deformation (L/L_0 between 0.9 and 0.7) appear to consist of four arcs, indicative of periodicities along the roll direction and the transverse diection. However, close inspection of the original negatives indicates the arcs along the roll direction are actually very weak and diffuse. As deformation by rolling continues, they become weaker and more diffuse until $L/L_0 = 0.5$, at which point they completely disappear. Therefore, up to this extent of roll, orientation occurs by the disappearance of one section of the diffraction ring, leaving only an arc along the transverse direction. As L/L_0 decreases below 0.5 two broad and somewhat diffuse meridional reflections are observed, indicating a periodicity of about 100 Å occurring along the roll direction. With further rolling, the intensity of these reflections increases relative to those along the transverse direction. The relative breadth and diffuseness of these new meridional reflections indicate that the periodicity which gives rise to the reflections may not be as uniform as the others; i.e. a greater deviation occurs in the spacing of these structural units.

As previously indicated, the general appearance of all of the SAXD patterns undergoes a discontinuous change at L/L_0 approximately equal to 0.4. For values of L/L_0 greater than 0.4 the maxima correspond to intensification of certain regions of the rings in the unoriented material. For lower values, a new periodicity is observed. Thus both the WAXD and SAXD indicate that abrupt, severe structural change(s) are occurring at an extent of roll of about 0.4 to 0.5.

As in the case of the WAXD data, pole figures have led to an interpretation of these complex patterns. Fig. 8 shows the SAXD pole figures of rolled POM as a function of L/L_0. (For these figures, the SAXD flat plate photographs sample the pole figure essentially along the circumference (beam along TH), equator (RD), and meridian (TD).) The predominant feature of these figures is the two maxima along the meridian, which give rise to the four-point patterns observed when the beam is parallel to the transverse direction (fig. 6). These maxima have, of course, two associated maxima on the other hemisphere of the pole figure. Each maximum then corresponds to one lobe of the four-point pattern and the angle β is the angle between the maxima.

Other features of the flat plate photographs can also be accounted for in the pole figure representation. The appearance of a four-point pattern, when the X-rays are parallel to the roll direction, corresponds to the two maxima along the equator ($L/L_0 = 0.5$) in fig. 8. The angle between these maxima is the angle α. The intensity along the equator begins to increase in the TH direction and then split as L/L_0 is decreased and reaches a maximum at about $\pm 45°$ from TH at $L/L_0 = 0.5$. At this stage of the deformation process, these maxima suddenly disappear leaving only the strong maxima along the meridian. The patterns with the beam in the TH direction are seen to result from the tails of the intensity distribution. Note that the 100 Å periodicity observed for $L/L_0 \leq 0.4$ is not shown in these pole figures.

The pole figures indicate that maximum lamellar orientation occurs at about $L/L_0 = 0.5$. At this extent of roll the intensity of the maxima are about ten times that of the minima. Further deformation, results in a decrease of the ratio of maximum to minimum intensity of the original spacing to eight.

The above results for the SAXD and WAXD textures of rolled POM are dependent, not only on the direction of the beam with respect to the sample, but also on the position of the roll surface with respect to the X-ray beam. Fig. 9 shows SAXD pole figures for a sample with

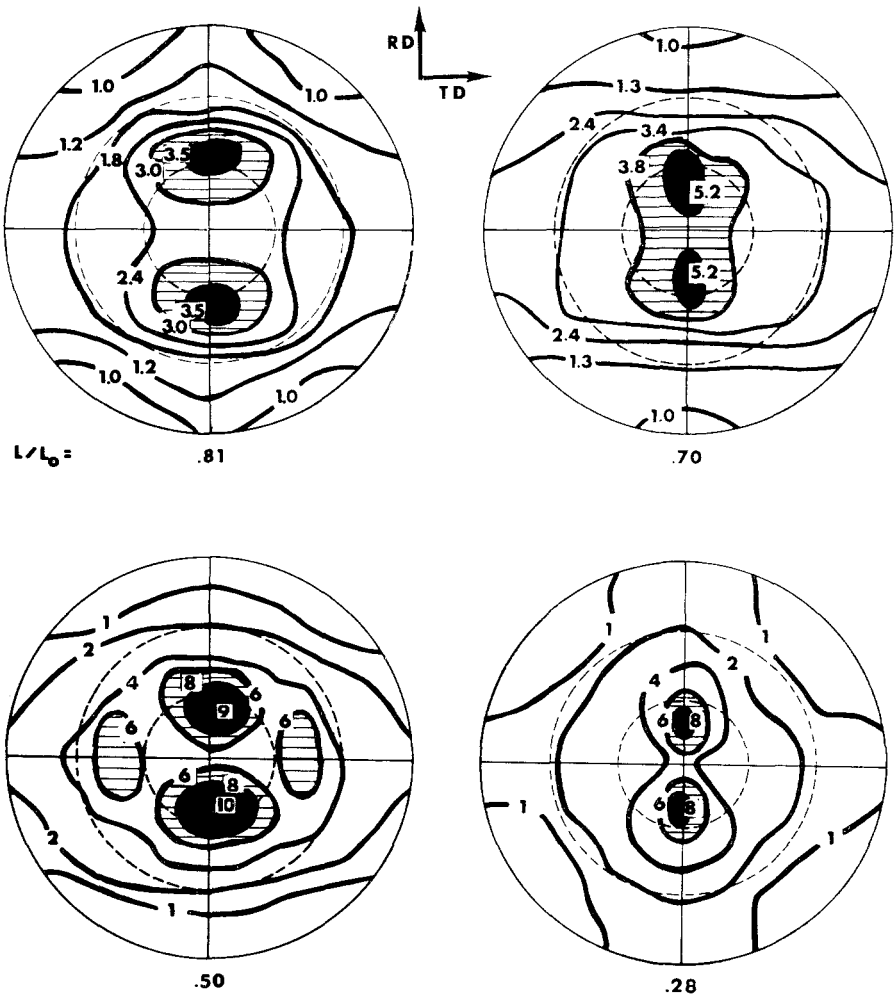

Figure 8 SAXD pole figures as a function of L/L_0.

$L/L_0 = 0.6$ taken at three different positions with respect to the roll surface. These pole figures were obtained by cutting the rolled slab into three sections: top, centre and bottom, and taking the pole figure of each separately. Note that the intensity of one maximum is 50 to 75% greater than the other maximum near the roll surfaces, while the centre of the sample yields maxima of equal intensity. The nearer to the centre of the specimen the beam strikes the sample the closer these maxima are to being equal in intensity, the pattern at the centre being symmetric. Note that this asymmetry is such that a mirror plane can be passed parallel to the roll surface through the centre of the sample. Similar pole figures were obtained for $L/L_0 = 0.4$. The SAXD patterns and pole figures indicate that the lamellae form a V-shaped pattern, with the points of the "V" lying on the centre plane of the sample and being closer to the front of the macroscopic specimen than the edges of the "V". (The front of the specimen is considered to be the side which is placed through the roller first.) This has also been shown to be true for unidirectionally rolled and annealed polyethylene [4]. One possible explanation for the appearance of asymmetry in uniaxially rolled, injection moulded POM is the presence of an initial surface orientation of the type described by Clark [28]. However, the presence of asymmetry in rolled, compression moulded POM as well as rolled PE [4], indicates that this asymmetry is due to the anisotropic nature of the rolling process rather than initial orientation.

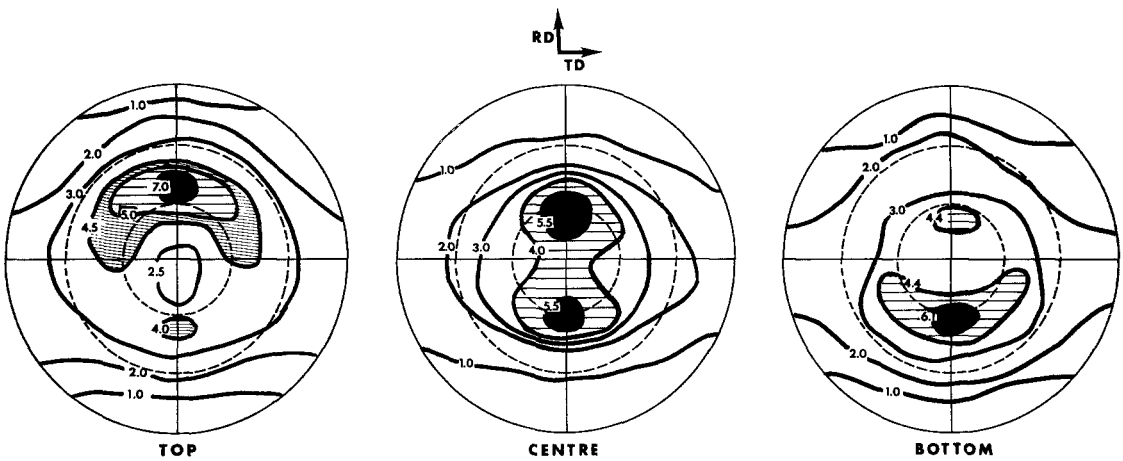

Figure 9 SAXD pole figures taken from three layers of a sample rolled to $L/L_0 = 0.6$.

3.4. Biaxial Rolling

The orientation effects in biaxially rolled POM are in some ways similar to those in uniaxially rolled POM. The four-point patterns observed along TD in uniaxially rolled samples are also present in biaxially rolled samples. However, in the latter case identical patterns are obtained when the beam is passed along either roll-direction. At low deformations with the beam in either RD, two arcs are seen along TH. With more severe deformation these arcs intensify at the ends and form a four-point pattern. Fig. 10 shows these small angle patterns at several extents of roll. Table II summarises the results of the measurements taken from these patterns. These data are placed in graphical form in fig. 11 for comparison with uniaxial rolling. As in the case of uniaxially rolled samples, the angle β decreases steadily as L/L_0 decreases, indicating that the lamellae tend to tilt toward the rolling plane as deformation increases. The small angle spacing also decreases steadily over the range observed, L/L_0 from 0.68 to 0.23. This is in contrast to the uniaxial case, where the spacing drops rapidly at about $L/L_0 = 0.5$. Thus, the severe and sudden structural changes which occur

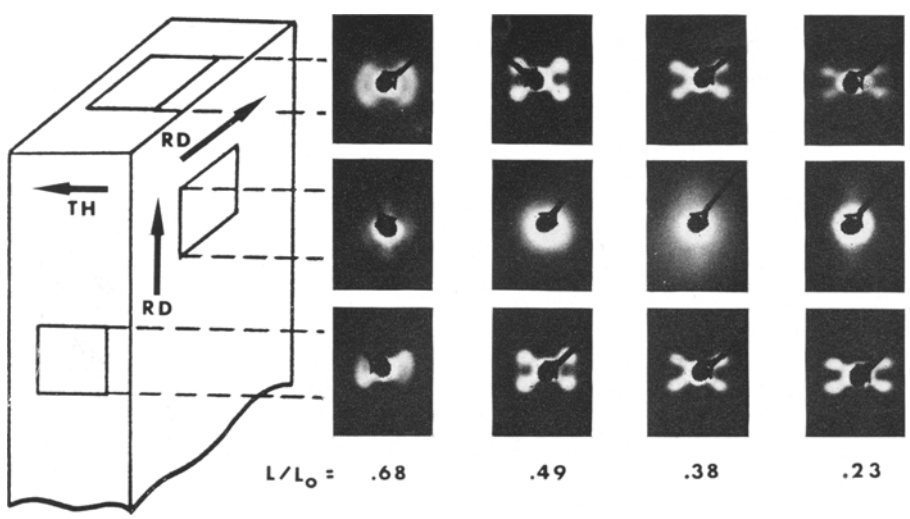

Figure 10 SAXD photographs of biaxially rolled POM.

TABLE II Observed small angle spacings for biaxially rolled POM

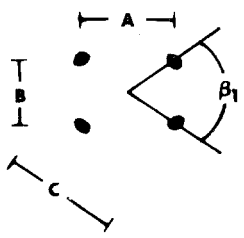

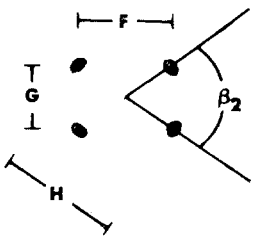

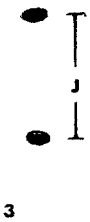

L/L_0	A	B	C	β_1	F	G	H	β_2	J
0.68	211	258	163	78°	208	294	165	73°	—
0.49	198	310	158	67°	203	315	160	66°	—
0.38	188	304	155	62°	184	304	154	61°	—
0.23	165	344	152	52°	165	338	145	50°	99

Columns 1, 2, and 3 correspond to the patterns in fig. 6 with the beam in the RD, TD and TH directions respectively The subcolumns A-J list Bragg spacings calculated from the reflections as defined in the sample patterns at the top of the columns; greek letters refer to the angles shown.

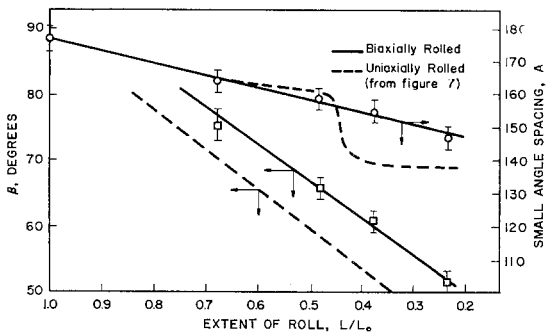

Figure 11 Effect of biaxial rolling on lamellar tilt and small angle spacing.

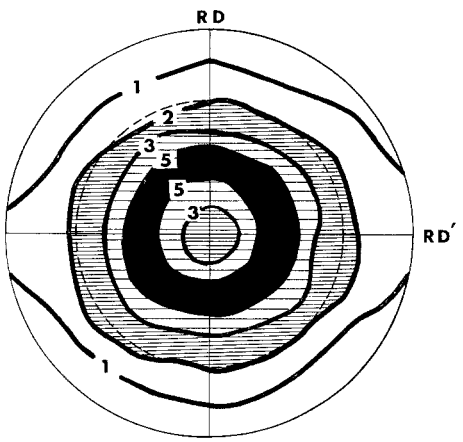

Figure 12 SAXD pole figure for biaxially rolled POM, $L/L_0 = 0.49$.

with uniaxial rolling at this point do not occur when samples are biaxially rolled.

The asymmetry observed near the roll surfaces of rolled POM is also present in biaxially rolled specimens, as can be seen in fig. 10 for $L/L_0 = 0.68$.

The question remains as to whether the four-point pattern in the biaxial samples indicates the presence of two distinct lamellar distributions, or a uniform distribution about TH of tilted lamellae. SAXD pole figures, one example of which is shown in fig. 12 ($L/L_0 = 0.5$), consist of one ring-shaped maximum indicating that the primary texture is one in which lamella normals make a constant angle ($\beta/2$ from Table II) with respect to the thickness direction. In this case the angle is 33°. This suggests that the lamellae lie so that they are tangential to the surface of a cone whose axis is perpendicular to the roll surface. Consequently, small angle diffraction should yield a four-point pattern independent of the direction of the X-ray beam, as long as the beam is parallel to the roll plane. This has been verified for several orientations and extents of roll.

WAXD pole figures for biaxially rolled POM indicate that a complex molecular orientation is also present. As before, the technique of assuming a certain molecular orientation, constructing a pole figure for the assumed orientation and then comparing the calculated and experimental figures must be applied. Fig. 13 shows the wide angle pole figures for biaxially rolled POM as a

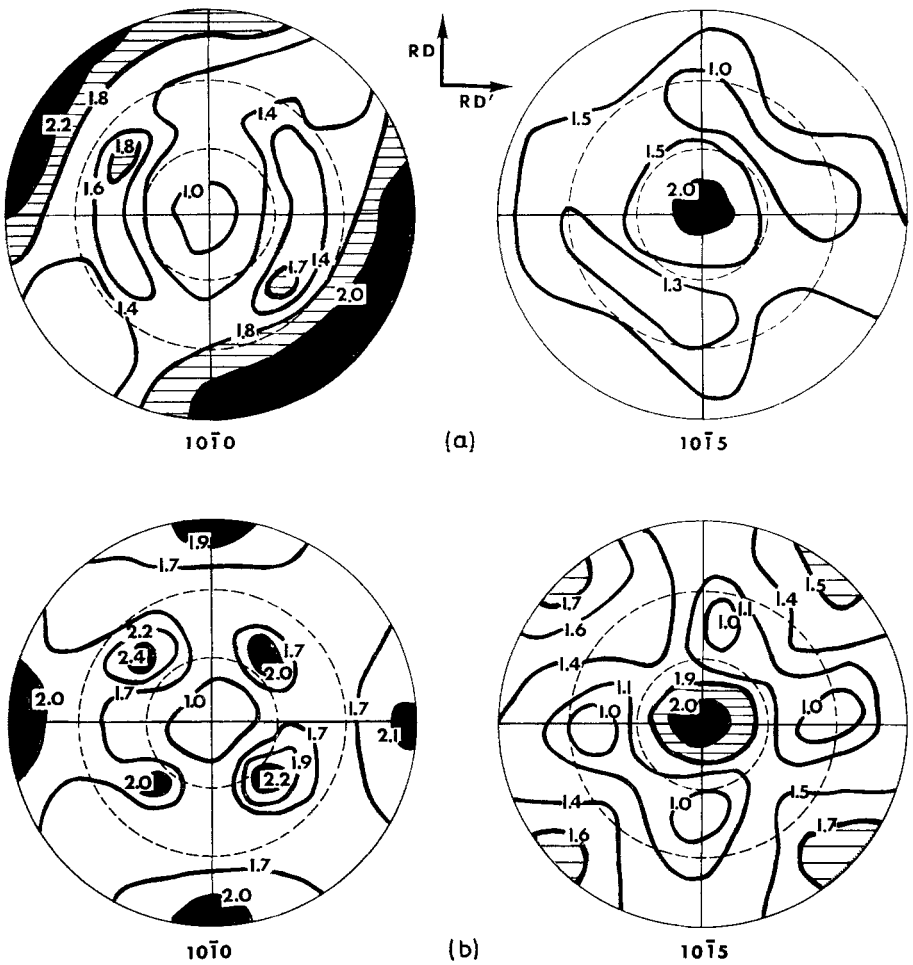

Figure 13

function of extent of roll. Very little definition can be observed up to an extent of roll of 0.68. Orientation, although present, seems to be very weak up to this point. As L/L_0 decreases to 0.49, eight maxima can be observed in the (10$\bar{1}$0) pole figure: two along each roll direction and four equally spaced at 45° to the roll directions and at about 40° to the sheet normal. The (10$\bar{1}$5) reflection is similar to that obtained from uniaxially rolled material, except for one subtle difference: the maxima along the circumference of the figure are equally spaced and at 45° to the roll directions. As L/L_0 is decreased further the figures change only slightly, the maxima on the meridian of the (10$\bar{1}$0) figure are reduced in intensity relative to the equatorial maxima and the circumference maxima of the (10$\bar{1}$5) figure shift slightly (5 to 15°) towards the meridian. This trend continues up to an extent of roll of 0.23. Here the meridional maxima observed in the (10$\bar{1}$0) figure are about half as intense as the equatorial maxima. Furthermore, the remaining four maxima are closer to the equator and are weaker. The (10$\bar{1}$5) pole at $L/L_0 = 0.23$ is similar to that obtained from uniaxially rolled POM.

As a model the orientation which occurs in the case of uniaxial rolling was used. It has been shown to consist of chains in the RD-TH plane and at $\pm$ 30° to the RD-TD plane with the *a*- and *b*-axes randomly oriented about the chain axis direction (fig. 4 and 5). If such a texture is placed along each roll direction, the result is a pattern that agrees quite well for biaxial rolling up to an extent of roll of 0.38. We will define such orientation here as "biaxial" orientation.

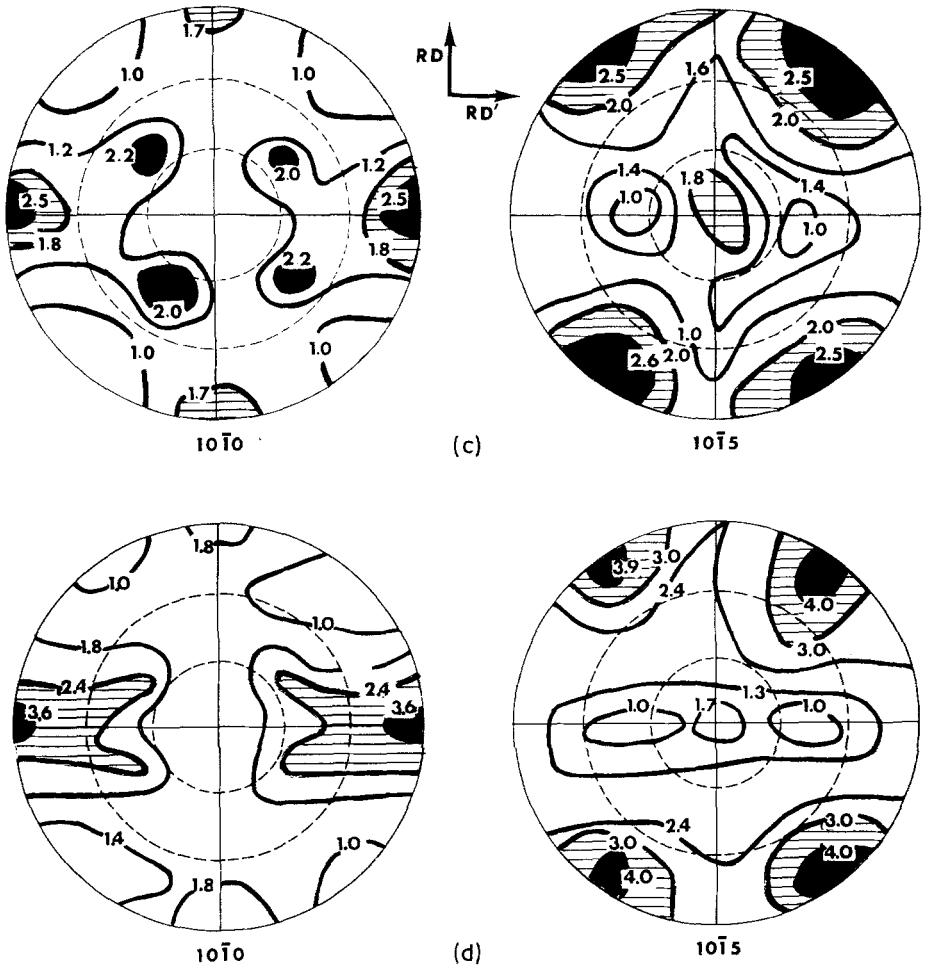

Figure 13 WAXD pole figures for biaxially rolled POM as a function of L/L_0. (a) $L/L_0 = 0.68$. (b) $L/L_0 = 0.49$. (c) $L/L_0 = 0.38$ (d) $L/L_0 = 0.23$.

The relative intensity of the meridional maxima with respect to the equatorial maxima will indicate how near to being truly "biaxial" the sample is. If the maxima are equal in intensity (approximately true for $L/L_0 = 0.49$ in fig. 13), the sample is truly biaxially oriented, i.e. the number of molecules at $\pm 30°$ to the first roll direction is the same as the number at $\pm 30°$ to the second. However, as L/L_0 is decreased, the meridional maxima decreases relative to the equatorial maxima. This indicates that chains are orienting preferentially at $\pm 30°$ to the RD direction rather than the RD' direction (where the RD direction is the direction of first advance of the material through the roller). At $L/L_0 = 0.23$ the pole figures take on a different character. The "RD population" is not only increasing in intensity relative to the "RD' population", but also, the chains are slowly tilting into the RD direction. The surprising aspect of this is that the molecules can remember and be influenced by the initial deformation, especially at high deformations.

3.5. Annealing of Uniaxially Rolled POM

Samples of rolled POM were annealed at various temperatures to determine the effect of heat treatment on the orientation. There is some dimensional recovery in all the samples, higher annealing temperatures tending to result in a greater increase in thickness than the lower temperatures.

Fig. 14 shows the SAXD patterns for various extents of roll and annealing conditions. The most striking feature of this series is the appearance of "six-point" patterns when the beam is in

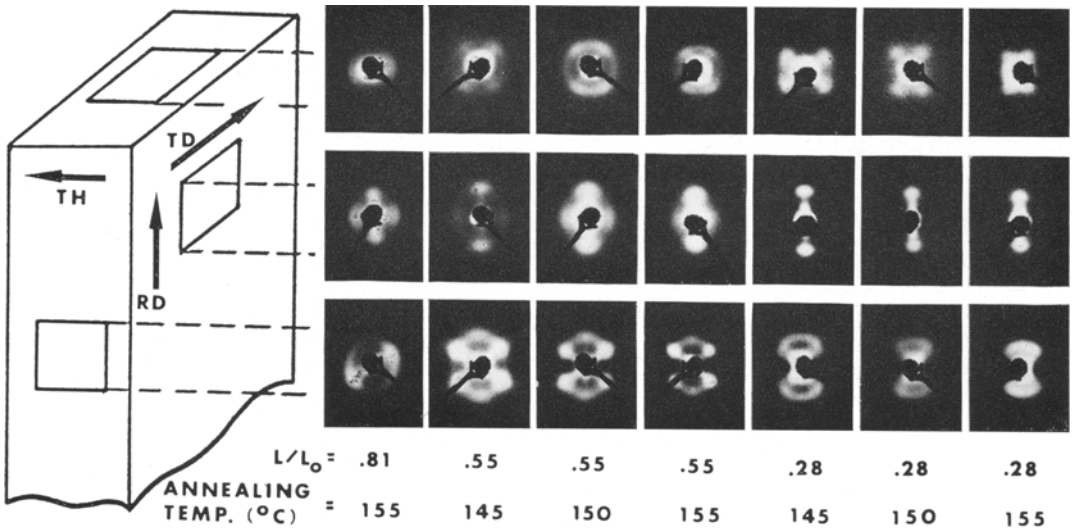

Figure 14 SAXD photographs for various extents of roll and annealing conditions.

the TD for annealed samples with L/L_0 between 0.8 and 0.45. Grossly similar patterns have been observed by O'Leary and Geil [7] in as-drawn POM. They attributed the meridional reflections to fibrous material and the reflections at $\pm 30°$ to the thickness direction to tilted lamellae. For annealed samples with L/L_0 less than 0.5, the intensity of the meridional reflection increases and the pattern begins to take on a "fan" shape. The effect of raising the annealing temperature at any given extent of roll is to decrease the size of the pattern, rather than change its shape. This indicates that two samples which have been deformed to the same extent of roll, but annealed at two different temperatures (within the ranges of temperatures studied here) will differ, not in lamellar orientation, but only in "long period". Annealing does not remove the surface asymmetry observed in rolled POM, as can be seen from fig. 14 for $L/L_0 = 0.81$, annealed at 155°C. Table III summarises the measurements from the small angle patterns.

The SAXD patterns of annealed POM can be roughly divided into two sections; L/L_0 (before annealing) less than 0.45 and L/L_0 greater than 0.45. Fig. 15 shows small angle pole figures for $L/L_0 = 0.28$ and $L/L_0 = 0.50$ annealed at several temperatures. Because of the greater variability of the "long period" in these samples, figures for $L/L_0 = 0.28$ were taken with the counter set at several values of 2θ.

The SAXD pole figure for $L/L_0 = 0.50$ annealed at 145°C (fig. 15a) shows in addition to the majority of the lamellae which now lie at an angle of about 40° to the roll direction some "transverse" orientation, i.e. as if lamellae were lying parallel to RD and at approximately $\pm 45°$ to TD. In addition, the ratio of maximum intensity to minimum intensity decreases with annealing (compare with fig. 18, $L/L_0 = 0.50$). The maxima which occur on the meridian move toward the roll direction, indicating that lamellae are tilting toward the TD-TH plane with heat treatment. The pole figures for $L/L_0 = 0.28$, annealed at 145°C, are shown for two different Bragg angles (figs. 15b and c). As 2θ is increased from 0.45 to 0.60°, the maxima which occur on the meridian shift from 32° to the roll direction to 17° to the roll direction. (Compare with fig. 8, $L/L_0 = 0.28$.) This accounts for the "fan" shaped pattern which occurs in these samples with the beam parallel to TD. Very weak equatorial maxima are also present in these figures. Fig. 15d shows the pole figure for a sample with $L/L_0 = 0.28$ annealed at 155° ($2\theta = 0.5$). Here meridional maxima occur indicating a periodicity along the roll direction, similar to that expected from a drawn fibre. (Changing 2θ for this sample has little effect on the overall appearance of the pole figures, except, of course, to decrease the absolute intensity of each data point.) However, a small amount of "transverse" orientation remains, as indicated by two weak maxima on either side of the meridian.

In contrast to the SAXD data which indicate

TABLE III Observed small angle spacings for POM at various rolling and annealing conditions

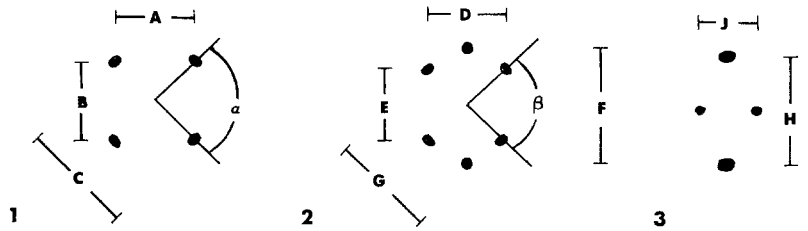

L/L_0	Annealing temperature (°C)	A	B	C	α	D	E	F	G	β	H	J
0.81	155			176 (w) (arc)		(w)	(w)		176 (w)		170 (w)	196
0.61	155	310 (w)	223 (w)	184 (w)	108°	239	275	170 (w)	185	81°	167	208
0.55	145	251	222	168	97°	193	274	136	158	70°	141	176
	150	297	228	172	101°	204	276	144	164	73°	168	203
	155	300	236	184	108°	291	275	156	180	80°	169	206
0.40	155	359	248	208	110°	214	253	158	166	80°	173	235 (w)
0.28	145	330	230	166	104°	244 (arc)		138	158	46°	139	178 (w)
	150	344	226	189	111°	264 (arc)		146	149	57°	154	198 (w)
	155	368	244	193	113°	290 (arc)		165	165	77°	171	(w)

w = weak reflection
Columns 1, 2, and 3 correspond to the patterns in fig. 4 with the beam in the RD, TD and TH directions respectively
The subcolumns A-J list Bragg spacings calculated from the reflections as defined in the sample patterns at the top of the columns; greek letters refer to the angles shown.

that much structural rearrangement at the 100 to 200 Å level is occurring during annealing. WAXD pole figures show that very little molecular rearrangement occurs. Fig. 16 shows a typical WAXD pole figure for an annealed specimen. This particular sample had an extent of roll of 0.50 and was annealed at 150°C. (Compare with fig. 4b.) The general shape of the pattern is similar to that of the unannealed sample, with the four maxima near the centre of the figure, indicating that the sample has more biaxial orientation than does the unannealed sample. Also, the ratio of maximum intensity to minimum intensity increases with annealing, indicating that the molecular orientation is somewhat stronger in the annealed samples for a given L/L_0.

3.6. Electron Microscopy

The dominant feature of the SAXD examination of rolled POM has been shown to be the four-point pattern with the beam along TD. There are several possible structural models which can explain this phenomenon, and consequently SAXD and WAXD analyses alone are not sufficient to identify the structural changes occurring during the rolling process. Although there remains some doubt about the quantitative correlation of the thickness of lamellae between electron micrographs and SAXD patterns in bulk polymers [29], electron microscopy can be used to complement the X-ray data qualitatively. Fig. 17 shows a Pt-C replica of a fracture surface of rolled POM ($L/L_0 = 0.8$). The sample was fractured such that the RD-TH plane was exposed. The fracture surface was then shadowed along RD. The SAXD pattern obtained from the same area with the beam perpendicular to the fracture surface is also shown. A "zig-zag" pattern of striations is characteristic of the surface. The width of these striations is 400 Å or greater, while the spacing calculated from the SAXD patterns is about 190 Å. Thus, these striations are probably stacks of lamellae rather than individual lamellae. The angle between the lamellae, β, as measured from the micrographs, ranges from 90 to 110°. β, as measured from the small angle pattern is 85°.

The lamellae tend to be aligned in bands parallel to the roll direction. These bands range

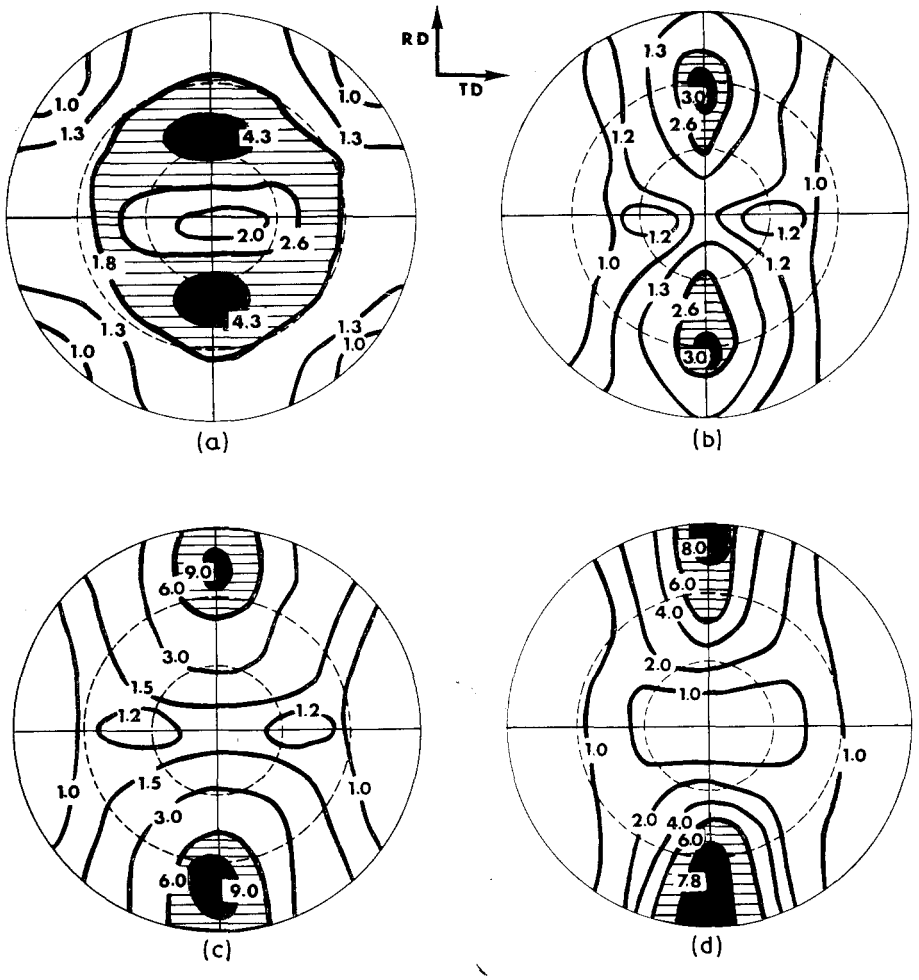

Figure 15 SAXD pole figures for $L/L_0 = 0.28$ and $L/L_0 = 0.50$. (a) $L/L_0 = 0.5, 2\theta = 0.50, 145°$ C. (b) $L/L_0 = 0.28, 2\theta = 0.45$. 145° C. (c) $L/L_0 = 0.28, 2\theta = 0.60, 145°$ C. (d) $L/L_0 = 0.28, 2\theta = 0.50, 155°$ C.

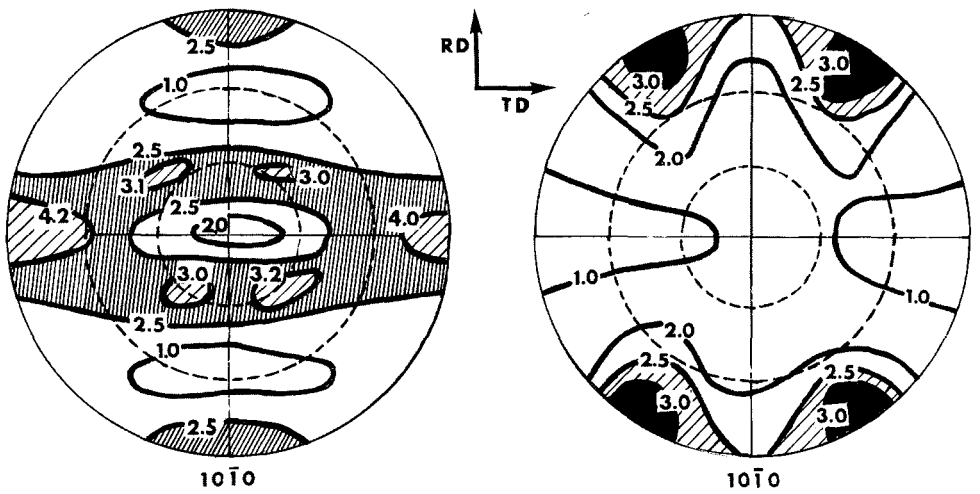

Figure 16 WAXD pole figures for uniaxially rolled POM. ($L/L_0{}^1 = 0.5$), annealed at 150° C.

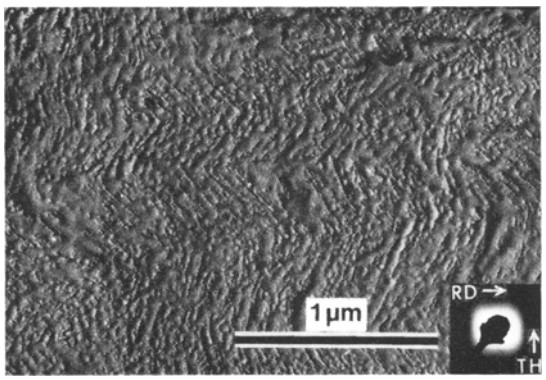

Figure 17 Electron micrograph of fracture surface of rolled POM, $L/L_0 = 0.8$.

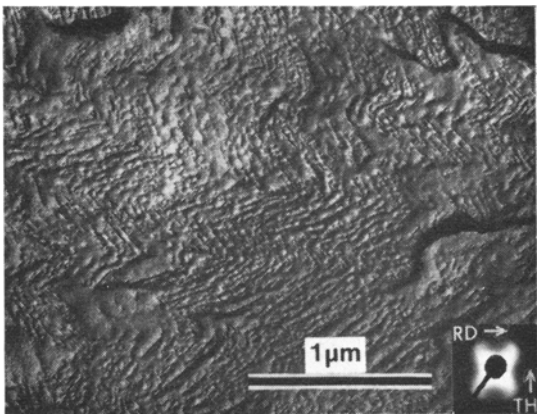

Figure 18 Electron micrograph of fracture surface of rolled POM, $L/L_0 = 0.7$.

from about 0.2 μm in lateral size up to about 25 μm. The appearance of this structure is very similar to the kink bands formed by compressing oriented polyethylene [16] and oriented nylon [30] along their fibre axes. This micrograph is representative of the structure observed over the entire fracture surface. However, many areas contain large sections which contain only one of the two orientations shown in fig. 17. Furthermore a few areas can be observed, especially in those samples with values of L/L_0 near one, where there is no appreciable orientation.

Fig. 18 shows a fracture surface in the RD-TH plane of a sample with $L/L_0 = 0.7$. The same banded, zig-zag structure occurs as in the case of $L/L_0 = 0.8$. In this case, the range of angles between lamellae is 75 to 90°, while β is 80° as measured from the four-point SAXD pattern shown in fig. 18. Again, areas are present in other regions of the same sample which contain only one of the two orientations observed, or a very few areas with no orientation at all.

A fracture surface and small angle pattern for a sample with $L/L_0 = 0.5$ are shown in fig. 19. Two definite lamellar orientations can again be observed occurring in bands more or less parallel to the roll direction. The range of the lamellar angles is 50 to 80° from the micrographs,while from the four-point pattern $\beta = 62°$. In contrast to the observations made on fracture surfaces of samples with L/L_0 nearer to one, the entire surface had this definite, banded, zig-zag structure. Furthermore, there is some indication that lamellar breakup may be starting at $L/L_0 = 0.5$ (arrows, fig. 19). Although some bands were larger than others, no areas were observed which contained only one of the two orientations.

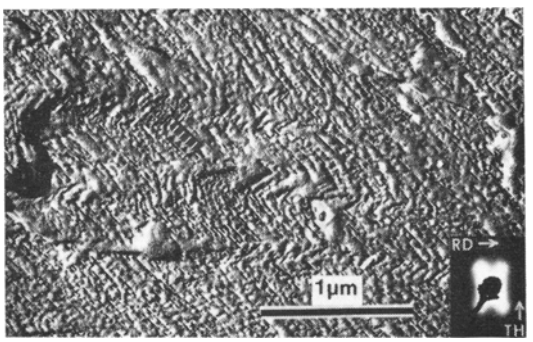

Figure 19 Electron micrograph of fracture surface of rolled POM, $L/L_0 = 0.5$.

These results show that as deformation by rolling is increased, lamellae (in large units) tend to tilt toward the roll direction and that more and more lamellae achieve this highly tilted conformation. The samples were scanned to see if a correlation between lamellar orientation and distance from the surface could be obtained. Such a correlation would be expected from the SAXD data (fig. 9). However, no statistically meaningful variations could be observed, probably because of the relatively small differences in orientation from edge to edge and the small areas over which the micrographs were taken.

Replicas of fracture surfaces of samples with L/L_0 less than 0.5 were difficult to obtain because the samples were extremely thin and would not fracture in the RD-TH plane. Instead, the material fractured in sheets more or less parallel to the RD-TD plane. These sheets may be related to the bands observed at lower deformation. A relatively even fracture surface of a sample with an extent

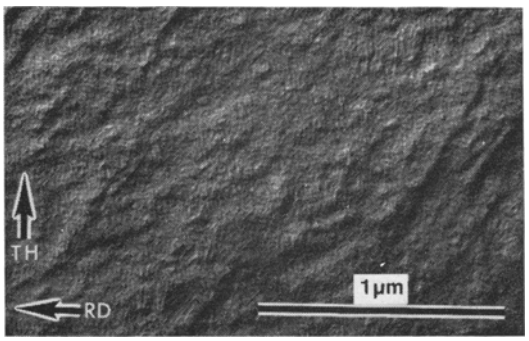

Figure 20 Electron micrograph of an annealed fracture surface of rolled POM, $L/L_0 = 0.28$.

of roll = 0.28 could be obtained by annealing the fractured samples at 150°C. Such a surface is shown in fig. 20. Note that the zig-zag banded structure observed in less deformed samples is not obtained. Instead, small lamellar-type structures about 200 Å in width and 400 to 1000 Å in lateral extent are observed, oriented nearly normal to the roll direction. These structures resemble those observed on free surfaces of drawn POM which has been annealed [31]. The bands remain, however, in annealed, rolled POM with $L/L_0 > 0.5$.

No observable orientation was obtained when any of the samples were fractured perpendicular to the roll direction.

4. Discussion and Interpretation

SAXD and WAXD data indicate that a complex series of structural changes occur during rolling. At low rolling deformation (L/L_0 from 1.0 to 0.5) the small angle "long period" decreases steadily with L/L_0 while the tilt of the molecular chains which have become oriented, with respect to the roll direction, remains at approximately 30°. As deformation is increased, a SAXD periodicity along RD of about 100 Å appears at an extent of roll of approximately 0.4. At the same extent of roll there is a sudden decrease in the spacing of the original structure (fig. 7). In addition, the molecular tilt decreases from 30° to RD, out of the rolling plane, to approximately 0° (fig. 4). In contrast to this, the angle between the lamellae, β, decreases linearly with extent of roll over the entire range of deformation (L/L_0 from 1.0 to 0.3). This indicates that at high rolling deformation either the molecules are nearly parallel (26°) to the lamellar surface or that some type of lamellar breakup is occurring. The latter explanation is preferred.

Fig. 21 represents a model suggested by the data. The lamellae tilt toward the roll direction, while the molecular chains remain at 30° to RD up to an extent of roll of 0.5. The molecular chains, therefore, must tilt within the lamellae as shown in fig. 21. Electron microscopy indicates that the lamellar tilt occurs in bands parallel to the roll direction (figs. 17 to 19). Thus, up to an extent of roll of 0.5, a model of oriented platelets, as described by Seto and Tajima [16], is suggested.

At an extent of roll near 0.5, the shear forces within the lamellae must increase as the molecules attempt to align in the roll direction. At this point the lamellae cannot remain as coherent units and tend to break up, possibly by a partial unfolding and large scale molecular slip. This mechanism may be similar to that described by Peterlin [32] for drawn polyethylene and O'Leary and Geil [7] for drawn POM. However, SAXD data indicate that the periodicity along RD is about 100 Å, whereas the model depicted in fig. 21 predicts a spacing approximately equal to the origin long period (177 Å). This indicates that some rearrangement other than simple unfolding and molecular slip must be occurring. Consequently, no attempt is made here to define the exact nature or mechanism of formation of these "blocks".

Although it is difficult to verify lamellar breakup directly via electron microscopy (fig. 19 shows some evidence of breakup, but this is far from conclusive), some macroscopic evidence is available. The highly deformed samples do not fracture evenly, instead, they fibrillate. Further, optical microscopy indicates that spherulite order is completely destroyed at this point.

Since the initial stages of the mechanism described above involves tilting of chains within lamellae, the long period should decrease with extent of roll according to

$$l = l_0 \sin\delta$$

where $l \equiv$ long period measured from SAXD at a given L/L_0, $l_0 \equiv$ long period of "as-moulded" material, and $\delta \equiv$ tilt of chains within lamellae ($\delta = 90°$ when chains are normal to the lamellar surface, as is presumably the case in the original sample). Table IV compares the observed long periods for uniaxial rolling (fig. 7) with those calculated from the above equation. The tilt of chains within the lamellae depends, of course, on two factors: tilt of chains with respect to the roll direction and tilt of lamellae with respect to the

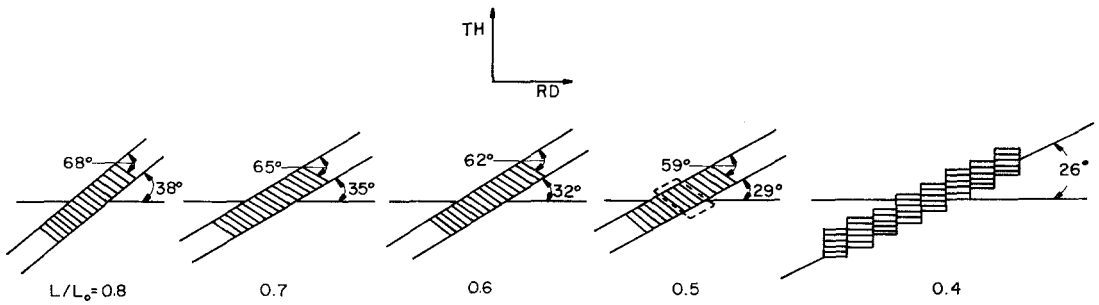

Figure 21 Schematic model indicating the effect of rolling on lamellar and chain tilt. Lamellar breakup is predominant at extents of roll less than 0.5.

roll direction, $\beta/2$. The calculated long periods are shown for two different values of chain tilt, 30 and 35°. Although WAXD pole figures indicate a tilt of about 30° a chain tilt of 35° seems to fit the observed data better than the 30° tilt. However, this disagreement is not unreasonable since the WAXD data were taken every 10°. Similar results were obtained using POM with an initial long period of 193 Å (as opposed to 177 Å in the above case). Again, a 35° chain tilt can explain the observed "d-spacing" decrease (table IV).

The observed and calculated long periods begin to diverge at $L/L_0 = 0.5$. Preliminary results suggest that the final spacing for $L/L_0 < 0.4$ depends only on rolling conditions (e.g. temperature) and not on the initial long period. A similar result has previously been reported by Peterlin and Corneliussen [33, 34] for drawn polyethylene.

For biaxially rolled samples table V compares the observed long period (fig. 14) with the calculated long period (assuming a 30° tilt of molecules with respect to the roll direction). This indicates that deformation occurs completely by lamellar tilting. Consequently, there is no evidence for the occurrence of lamellar breakup in the case of biaxial rolling to the extent used here. Again, macroscopic properties of the rolled material verify this, in that these samples will fracture down to $L/L_0 = 0.2$.

Consideration must now be given to the mechanism by which the molecules tilt within the lamellae. The expected slip system for POM is $(10\bar{1}0)$ [0001]. This allows the $(10\bar{1}0)$ planes, which are the most densely packed (hki0) planes, to act as slip planes. Since the lamellae must retain their crystal structure one might expect slip to occur in steps of the c-spacing. Using the model of Hansen and Rusnock [35],

TABLE IV Calculated and observed small angle spacings for uniaxially rolled POM

L/L_0	Observed long period (A)	Calculated long period (for 30° chain tilt with respect to R) (A)	Calculated long period (for 35° chain tilt with respect to R) (A)
1.0	177	—	—
0.8	171	164	169
0.7	165	160	166
0.6	162	156	163
0.5	160	152	159
1.0	193	—	—
0.8	188	184	189
0.7	186	181	186
0.6	184	176	182
0.5	181	168	177

TABLE V Calculated and observed small angle spacing for biaxially rolled POM

L/L_0	Observed long period (A)	Calculated long period (for 30° chain tilt with respect to R) (A)
1.0	177	—
0.65	165	164
0.5	158	158
0.35	153	153
0.2	147	145

involving uniform tilt and c-axis spacing slip of the molecules, the angle the molecule makes with the stress direction is given by;

$$\theta = \tan^{-1} d_{(10\bar{1}0)}/nd_{(0001)}$$

where n is the number of c-spacing slips per plane and the draw ratio $= 1/\sin\theta$. For the above slip system in POM $\theta = 12°$ (for $n = 1$), and the draw ratio = 4.6. (Because of the large c-spacing of POM (17.3 Å), relative to a and b, these

values do not change significantly for other possible (hki0) [0001] slip systems.)

This suggests that those chains participating in the deformation tilt to within at least 12° of the roll direction. However, as observed here, and in the case of uniaxial drawing of POM [7] the chains at first tilt at a 30° angle. Therefore we conclude that the model of Hansen and Rusnock cannot lead to a direct explanation of the observed 30° tilt.

The relationship between the initial spherulitic order and lamellar orientation after rolling is a matter of some speculation, since little direct data are available. Initially, the material has been shown to be composed of spherulites with a systematic distribution but an overall random orientation of lamellae. It is difficult to tell exactly what happens during rolling to any one lamella with a given orientation. This situation is further complicated by the fact that the lamellae cannot react to the deformation independently, since they are joined by tie molecules [36-38]. Thus, co-operative motion must be present in regions of the spherulites. This is borne out by the electron micrographs shown in figs. 17-19. However, it is difficult to envisage a mechanism whereby portions of a band of tilted lamellae will suddenly reverse their tilt, leading to the observed decrease in width of the bands at high deformation.

Various regions of a spherulite would be expected to react differently to deformation as pointed out by Oda, Nomura, and Kawai [30] and O'Leary and Geil [7]. They divided spherulites into four regions (two lateral zones and two longitudinal zones), by means of two diagonals along lines of maximum shear stress (45° to the draw direction). The lamellae in the lateral zones are expected to react differently during deformation than those in the longitudinal zones.

The work by the above authors was concerned with deformation by an applied tensile load. However, rolling is similar to drawing in that the tangential (frictional) force of the roller provides a component which exerts a tensile stress on the material [5]. Therefore, rolling can be considered to be a combination of drawing along the roll direction and compression along the thickness direction.

O'Leary and Geil [7], using pole figure analysis, have shown that at low draw ratios (35 to 125%) the chains are preferentially tilted at $\pm$ 30° about both the thickness and transverse directions, directions which are equivalent for drawing. However, for rolling, these directions are not equivalent and one degree of freedom is lost. Thus our results agree in that the chains are tilted $\pm$ 30° about the transverse direction.

The SAXD pole figures indicate a relatively high intensity of poles parallel to TH (fig. 8); this orientation can be explained as follows. A lamella which lies initially in the rolling plane has no net moment associated with it tending to tilt it out of the plane. The only force on this lamella would be that due to its (longer range) association with lamellae (via tie molecules) which are tilted out of the rolling plane. This force would be of less consequence than for a lamella which has a direct moment applied to it. In this vein, then, we suggest that the results of rolling can be thought of in the following way: the lamellae, which lie at angles to the rolling plane greater than that of preferred tilt, tend to rotate in order to approach the preferred tilt. On the other hand, lamellae with less than the preferred tilt are affected very little.

WAXD and SAXD pole figures obtained from biaxially rolled POM seem, at first glance, to be contradictory. WAXD pole figures indicate that the molecules preferentially lie at $\pm$ 30° to each of the two roll directions. Thus, two distinct molecular orientations exist. In contrast to this, SAXD pole figures indicate a nearly continuous distribution of lamellae lying on the surface of a cone. This anomaly can be resolved by considering the SAXD pole figure (fig. 12) to be composed of four maxima, two on the meridian and two on the equator. Because of the breadth of these two distributions, it may be that we are not able to resolve the individual poles, and the maxima appear continuous. (Another possibility is that chains can tilt various ways with respect to a given lamella.) Thus, in some ways, biaxial rolling can be considered to be a superposition of the two structures obtained by uniaxial rolling in the two rolling directions. However, the lamellar tilts do not coincide for a given extent of roll (fig. 11). For example, at $L/L_0 = 0.5$, the lamellar tilt = 29° for uniaxial rolling, while for biaxial rolling the lamellar tilt = 34°. This indicates that deformation due to biaxial rolling may not be as severe as that of uniaxial rolling. Consequently, deformation can occur by lamellar tilting even to $L/L_0 = 0.2$. The tilt of chains with respect to lamellae at this point is about 56°, which is approximately the angle at which the lamellae begin to break up during uniaxial

rolling. Presumably, lamellar breakup would occur if biaxially rolled films could be rolled beyond this point.

On the basis of the results from biaxially rolled samples, the four-point SAXD pattern obtained in uniaxially rolled samples with the beam parallel to RD can now be explained. It has been shown that an increase of lateral dimension occurs upon uniaxial rolling (fig. 3). If it is assumed that the entire increase in this dimension is due to a form of biaxial deformation, the increase in width at $L/L_0 = 0.48$ corresponds to an extent of roll of about 0.81 (fig. 3), i.e. uniaxial rolling to $L/L_0 = 0.81$ would give about the same increase in dimension. Comparing the four-point patterns obtained in each of the two cases ($L/L_0 = 0.48$ along RD; $L/L_0 = 0.81$ along TD), they are found to be nearly identical ($\alpha = 79°$; $\beta = 78°$). Thus, this seemingly anomalous four-point pattern is a result of the increase in width of the uniaxially rolled samples. It is conceivable, then, that the maxima on the meridian of the $(10\bar{1}0)$ WAXD pole figures (fig. 3) represents the chains which are within those lamellae giving rise to this secondary four-point pattern. In this sense WAXD and SAXD are consistent, i.e. a small amount of "biaxial" deformation is present on both the molecular and super-molecular scales.

Aside from the small amount of "biaxial" deformation in uniaxially rolled POM, this deformation process has been shown (at least at low deformations) to consist of lamellar tilt in bands parallel to the roll direction. This tilting is probably due to a combination of tensile and normal forces exerted by the roller. However, a further variable is added since a shear stress distribution exists within the sample. This distribution is such that the maximum shear stress occurs at the roll surface and the maximum velocity occurs at the sample centre. (This latter phenomenon manifests itself in the fact that the centre of the leading edge of the sample bulges slightly.) Consequently, the edge of a given lamellae which is nearer the centre of the specimen will tend to move slightly faster than the outer edge. This, superimposed on the tension and compression discussed earlier, presumably gives rise to the asymmetry observed in rolled POM. The importance of the shear stress distribution relative to the absolute magnitude of the forces involved will determine how asymmetric the specimen is. For example, the smaller pair of maxima for rolled and annealed low density PE are too weak to be observed in some cases [4].

The most surprising feature of the results of annealing is that lamellar orientation changes significantly, while little change is observed in molecular orientation. For example, comparing tables I and IV for $L/L_0 = 0.55$, the lamellar tilt ($\beta/2$) for the unannealed sample is about 30°, while $\beta/2 = 40°$ when the sample is annealed at 155°C. In contrast to this, the molecular tilt remains at about 30° to the roll direction. This indicates that the effect of annealing is to rotate the lamellae so as to increase the angle (δ) between the lamellar surface and the chain axis. δ will, therefore, approach its more natural value of 90°. In the case mentioned above δ increases from 60 to 70° with annealing. In addition, the annealing experiments (fig. 14) indicate that the lamellar breakup, leading to a fibrous component (meridional reflection of the six-point SAXD pattern), may be occurring to a small extent even at low deformations.

The effect of rolling on the yield properties of polymers seems to be quite general, i.e. the yield stress is increased in the direction of rolling and is decreased in the transverse direction. However, specific details (strain to break, breadth of the yield region, etc.) depend on the polymer in question. Because little structural work has been reported on rolled polymers previously discussed in the literature, it is difficult to say why POM reacts differently, with regard to strain to break, from these polymers. On the other hand, it can be shown that the tensile properties of POM are consistent with the structural results discussed previously.

When rolled POM is drawn along the roll direction, it line-draws until all the material is fully drawn. Then, and only then, will the sample break. On the other hand the material tends to break after yield and during line-drawing, when drawn perpendicular to the roll direction. This break always occurs at that portion of the tensile specimen which is then undergoing deformation, i.e. at the neck.

A tensile stress, placed along the roll direction is nearly parallel (30°) to the molecules (and presumably tie molecules between lamellae). Consequently, it would be difficult for a crack to propagate perpendicular to this direction. The molecules can then rotate (30°) into the direction of strain in order to relieve the imposed stress. At this point lamellar order is lost (no SAXD spacing can be observed from about 15% strain

to about 30% strain, where a fibre pattern is observed) and yielding occurs. However, a stress placed in the transverse direction is perpendicular to the molecules (and tie molecules). Cracks can now easily propagate perpendicular to the applied stress. It now becomes a question of whether chains are able to rotate a full 90° into the stress direction before crack propagation and catastrophic failure can occur.

Acknowledgement

This research was supported, in part, by the National Science Foundation and by a Public Health Service Career Development Award (to PHG).

References

1. I. L. HAY and A. KELLER, *J. Mater. Sci.* **1** (1966) 41.
2. *Idem, ibid* **2** (1967) 538.
3. F. C. FRANK, A. KELLER, and A. O'CONNOR, *Phil. Mag.* **3** (1958) 64.
4. J. J. POINT, D. M. GEZOVICH, A. KELLER, and G. A. HOMES, *J. Mater. Sci.*, in print.
5. W. WILCHINSKY, *J. Appl. Polymer. Sci.* **7** (1963) 923.
6. *Idem, J. Appl. Phys.* **31** (1960) 1969.
7. K. O'LEARY and P. H. GEIL, *J. Macromol. Sci. (Phys.)* **B2(2)** (1968) 261.
8. G. S. Y. YEH and P. H. GEIL, *ibid* **B1(2)** (1967) 251.
9. W. O. STATTON and G. M. GODARD, *J. Appl. Phys.* **28** (1957) 1111.
10. E. W. FISCHER, H. GODDAR, and G. F. SCHMIDT, *Kolloid Z. u. Z. Polymere* **226** (1968) 30.
11. W. O. STATTON, *J. Polymer Sci.* **41** (1959) 143.
12. K. HESS and H. KIESSIG, *Z. Physik. Chem.* **193** (1944) 196.
13. L. B. MORGAN, *J. Appl. Chem.* **4** (1954) 160.
14. R. BONART and R. HOSEMANN, *Inter. Union Pure Appl. Chem.* Symposium on Micromolecular Chemistry, preprints paper **IB9** (1959).
15. T. SETO, and T. HARA, Reports on Progress in Polymer Physics IX (Japan 1966).
16. T. SETO and Y. TAJIMA, *J. Appl. Phys. Japan* **5** (1967) 534.
17. R. BONART, *Kolloid Z. u. Z, Polymere* **199** (1964) 136.
18. W. WILCHINSKY, *Soc. Plastics Engin. Jour.* **22** (1966) 46.
19. I. SWERLICH and F. P. GAY, U.S. Patent No. 2,952,878, Sept. 20, 1960.
20. J. G. WILLIAMS and H. FORD, *J. Mech. Eng. Sci.* **9** (1967) 362.
21. G. GRUENWALD, *Modern Plastics* **38** (1960) 137.
22. A. KELLER and J. G. RIDER, *J. Mater. Sci.* **1** (1966) 389.
23. B. MAXWELL and P. H. ROTSCHILD, *J. Appl. Polymer. Sci.* **5** (1961) S11.
24. A. PETERLIN and J. ELWELL, *J. Mater. Sci.* **2** (1967) 1.
25. L. J. BROUTMAN and S. KALPAKJIAN, SPE 27th Annual Technical Conference, Chicago, Ill., May 1969.
26. B. D. CULLITY, "Elements of X-ray Diffraction," Addison-Wesley Pub. Co., Reading, Mass. (1959) 285.
27. D. M. GEZOVICH, Ph.D. Thesis, Case Western Reserve Univ. (1969).
28. E. S. CLARK, *Soc. Plastics Engin. Jour.* **23** (1967) 46.
29. P. H. GEIL, *J. Polymer Sci.* Part C **13** (1966) 149.
30. D. A. ZAUKELIES, *J. Appl. Phys.* **33** (1962) 2797.
31. A. SIEGMANN and P. H. GEIL, *J. Macromol. Sci. (Phys.)* in print.
32. A. PETERLIN, *J. Polymer Sci.*, Part C, **15** (1966) 427.
33. R. CORNELIUSSEN and A. PETERLIN, *Makromol. Chem.* **105** (1967) 193.
34. A. PETERLIN, and R. CORNELIUSSEN, *J. Polymer Sci.* A-2, **6** (1968) 1273.
35. D. HANSEN and J. A. RUSNOCK, *J. Appl. Phys.* **36** (1965) 332.
36. I. HAY and A. KELLER, *Kolloid Z.* **204** (1965) 43.
37. V. F. HOLLAND and P. H. LINDENMEYER, *J. Appl. Phys.* **36** (1965) 3049.
38. R. BONART, *Kolloid Z.* **199** (1964) 136.
39. T. ODA, S. NOMURA, and H. KAWAI, *J. Polymer Sci.* A3 (1965) 1943.

Received 7 October 1970 and accepted 8 March 1971